Available online at www.sciencedirect.com
SCIENCE DIRECT®
Journal of Nuclear Materials 342 (2005) 14–19
journal of nuclear materials
www.elsevier.com/locate/jnucmat

Analysis of controversial zones of the Zr–Cr equilibrium diagram

R.O. González [a,*], L.M. Gribaudo [a,b]

[a] Departamento Materiales, Centro Atómico Constituyentes, Comisión Nacional de Energía Atómica, Avda. Gral. Paz 1499, B1650KNA San Martín, Argentina
[b] Consejo Nacional de Investigaciones Científicas y Tecnológicas, Avda. Rivadavia 1917, C1033AAJ Buenos Aires, Argentina

Received 5 January 2005; accepted 19 March 2005

Abstract

Zr–Cr alloys were fabricated in an arc furnace by melting pure chromium and zirconium containing two different concentrations of oxygen. Isothermal heat treatments were performed in the range from 840 to 960 °C. The chromium compositions were selected in order to establish equilibria and transformation temperatures near the eutectoid zone and to determine the eutectic reaction in the zirconium rich zone. Phase characterizations and determination of their compositions were carried out by metallographic observations, X-ray diffraction and electron microprobe analysis. Transformation temperatures were obtained measuring the resistivity by the four-point method and by differential thermal analysis. The conditions of the eutectoid and eutectic invariant transformations and general sketches of equilibria in the zirconium-rich zone of the Zr–Cr–O system could be outlined at different temperatures. From the results obtained, $\beta(X_{Cr} \sim 1.3$ at.%) $\leftrightarrow \alpha(X_{Cr} \leqslant 0.1$ at.%) + α-$ZrCr_2$ at $T = 840$ °C and $L(X_{Cr} = 26.5$ at.%) $\leftrightarrow \beta(X_{Cr} \sim 4.7$ at.%) + α-$ZrCr_2$ at $T = 1380$ °C.

1. Introduction

Many critical components for nuclear power reactors are manufactured employing zirconium-base alloys. Chromium, in contents of about 0.1 wt% Cr, is a current constitutive element in Zircaloy-2 and Zircaloy-4 alloys. Published experimental data on phase equilibria in the Zr–Cr system are relatively abundant. The system has been critically assessed in [1] where a complete provisional equilibrium phase diagram was proposed. This diagram was later reproduced in [2].

Previous thermodynamic phase modelling of this binary system considering $ZrCr_2$ as a line compound was presented in [3]. Other models involving the polymorphism of the intermetallic phases, (cF24 α-$ZrCr_2$, hP24 β-$ZrCr_2$ and hP12 γ-$ZrCr_2$) and their compositional extensions, were further suggested in [4] and [5]. A new proposal of the Zr–Cr phase diagram was presented in [6] taking into account results of computed equilibria after modelling in [4]. Some differences can be observed in the zirconium-rich zone of these proposals involving the invariant eutectoid and eutectic equilibria. The motivation of the present work was to elucidate these topics.

On the other hand, phase equilibria in the global ternary Zr–Cr–O have been investigated at 1200, 1500 and 1700 °C in [7] and on the zirconium-rich zone only at

* Corresponding author. Fax: +54 11 6772 7269.
E-mail address: rugonz@cnea.gov.ar (R.O. González).

0022-3115/$ - see front matter © 2005 Elsevier B.V. All rights reserved.
doi:10.1016/j.jnucmat.2005.03.014

850, 890, 920 and 950 °C in [8]. While chromium has a moderate effect in promoting the formation of cubic β-Zr, oxygen strongly stabilises the hexagonal α-phase. The influence of adding oxygen to the binary Zr–Cr system is here considered taking into account two different contents in the original zirconium metal used for the fabrication of the alloys.

2. Experimental details

Alloys were prepared by melting the metal components in a non-consumable tungsten electrode arc furnace with a copper crucible under a high purity argon atmosphere. Zirconium 99.8 wt% (1100 wt.ppm or 0.62 at.% O) of nuclear purity, zirconium from Oremet-Wah Chang company 99.85 wt% (420 wt.ppm or 0.24 at.% O) and chromium of at least 99.85 wt% (50 ppm Fe as the main impurity) purity were used. The chromium compositions of the alloys were as follows: 0.3, 1, 2, 4, 15, 26 and 26.5 at.%. They were labelled N0.3, W0.3, N1,W1, N2, W2, N4, W4, N15, W15, W26 and W26.5 according to each kind of zirconium used (N for nuclear quality, W for Oremet-Wah Chang) and to their corresponding chromium compositions (in at.%).

Specimens of alloys containing from 0.3 to 4 at.% Cr were heat-treated at $T = 840$, 860, 900 and 960 °C during 1000 h. In order to perform the heat treatments, the labelled specimens were wrapped in tantalum foils, encapsulated in quartz tubes under argon atmosphere and placed in a conventional horizontal furnace with a highly accurate temperature control device (±2°C). Quartz tubes containing the specimens were finally quenched in water at room temperature. Specimens from 15 to 26.5 at.% Cr were especially made to study the eutectic transformation.

Samples of the alloys were suitably polished and etched by means of a water solution of HNO_3 and HF (45:5:50 vol.%). Phase characterizations were firstly performed by optical microscopy in a Reichert-MEF II microscope (OM). Phase compositions were determined by quantitative microanalysis (EPMA) with an electron microprobe equipment CAMECA SX-50. Quantitative compositional microanalysis was performed under an accelerating potential of 20 kV. The equipment was recalibrated before each analysis session using pure 99.99 wt% Zr and 99.999 wt% Cr standards. Total oxygen was measured by gas chromatography on some alloy samples after heat treatments using a Leco TC-36 analyzer. The specimens acquired about 0.17 atO % (300 ppm). This amount was added to the initial quantity present in the zirconium composing these alloys in order to consider the actual composition in the alloys.

With the aim of determining the solid transformation temperatures, electrical resistance vs. temperature measurements (RM) on polycrystalline strips (about $2 \times 0.15 \times 40$ mm^3) of the alloys were performed in a suitable equipment, able to maintain a vacuum of about 10^{-8} bar. The four-point method was employed, heating and cooling at 3 °C/min. A typical curve ρ/ρ_0 ($\rho_0 = \rho_{max}$ for normalization) vs. T, obtained on W1 alloy, is shown in Fig. 1. It was considered that the maximum value of resistivity in heating determines $T(\alpha \rightarrow \alpha + \beta)$ when α begins to disappear, and the intersection of tangents of the subsequent sections of the curve $T(\beta \rightarrow \alpha + \beta)$ when α has totally disappeared [9].

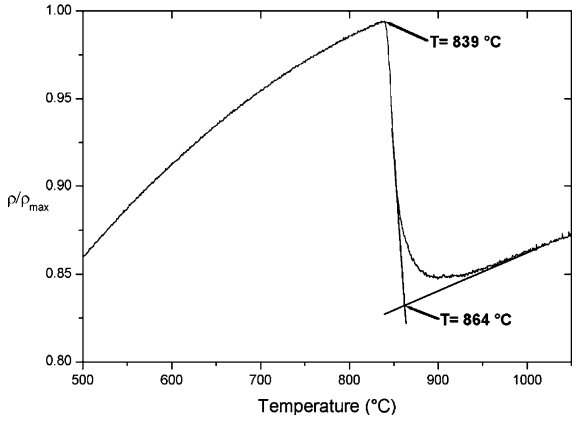

Fig. 1. Typical resistivity vs. temperature curve during heating obtained on W1 alloy.

Differential thermal analysis (DTA) was performed on W15, W26 and W26.5 alloys on specimens of about 0.1 g in a Shimadzu DTA-50 equipment using alumina crucibles. The point at the beginning of the peaks in heating at rates of 10 and 20 °C/min were considered as the transformation temperatures. Corrections of the transformation temperatures were performed extrapolating the onset temperatures to a rate of 0 °C/min, linearly for the eutectic and following the method suggested in [10], which considers diffusion of the elements in the solid phases, for the eutectoid transformation.

Characterization of phases in some selected specimens was also performed from X-ray diffraction patterns (XRD) using monochromatic CuKα radiation in an X-ray PW3710 Philips equipment. Analysis of the diffractograms of massive or powder samples were carried out using the PCw program [11]. Lattice parameters and mass percentages of phases were estimated.

3. Results and discussion

3.1. Zirconium-rich zone

Fig. 2 shows optical micrograph N4 alloy heat treated at 860 °C. This type of microstructure is typical of

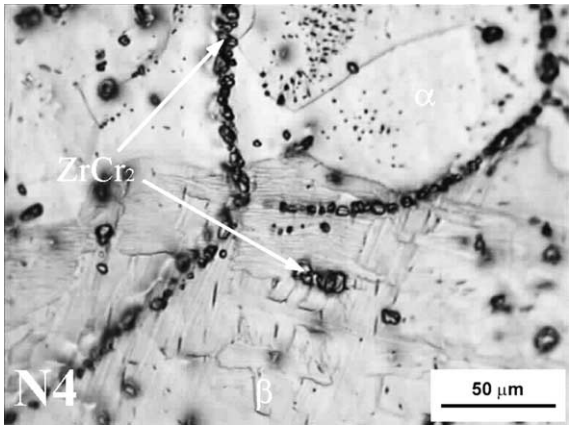

Fig. 2. Microstructure of N4 alloy after heat-treatment at 860 °C.

a ternary equilibrium. Three different phases can be observed: α and β' solid solutions and α-$ZrCr_2$ intermetallic. Both solid solutions, α and β', have the hcp zirconium structure differing in the chromium concentration. The β' phase is formed by fast cooling during quenching after the heat treatments and has a chromium concentration corresponding to the β bcc structure at the equilibrium temperature.

Tables 1 and 2 present the phases in equilibrium characterized at each temperature for the two series of alloys with chromium contents from 0.3 to 4 at.%. Chromium compositions measured by EPMA are also included. Partial isothermal sections of the equilibrium diagram of the ternary Zr–Cr–O system in the zirconium rich zone, considering some hypothesis, can be deduced.

Fig. 3 presents partial isothermal sections showing phase equilibria in the zirconium rich zone of the ternary Zr–Cr–O system which are outlined after considering the following hypotheses: (1) The total oxygen contents of the alloys (0.41 and 0.79 at.% for the W and N series, respectively) are taken as the amount in the original zirconium (0.24 or 0.62 at.%) with the addition of 0.17 at.% O (estimated amount which was added during the fabrication and the heat-treatments). (2) Mass balances for all the components in each phase and some other simplifications, i.e. oxygen insolubility in α-$ZrCr_2$, etc., allowed to calculate tie-lines and equilibrium triangles for bi- and monovariant transformations and to draw plausible phase boundaries. Comparing these sections with the similar sections proposed in [8], only some little differences can be found, specially in the 850 °C section of that work related to the 860 °C section here presented.

After examining these results a conclusion about the phase compositions in the eutectoid transformation could be outlined. Chromium atomic percentage at the eutectoid temperature is lower than 0.1 at.% for the α phase and about 1.3 at.% for the β phase.

3.2. Eutectoid transformation

Table 3 presents results of the resistivity measurements. The first column shows the temperature at which the resistivity value stops rising during heating indicating the moment when the α phase begins to disappear. In the second column, the temperature obtained by intersections of the tangents of the resistivity curves, indicates that the α phase has totally disappeared. In the third column, a slight singularity of the curve which is appreciated only in W2, W4, N2 and N4 alloys, could be interpreted as the temperature at which the intermetallic disappears. Analyzing the results of the first column for both W and N alloy series $T(\beta \leftrightarrow \alpha + \alpha\text{-}ZrCr_2) = 840$ °C is suggested.

The onset temperatures determined through the differential thermal analysis in W15 alloy were 884.6 and 897.4 °C at heating rates of 10 and 20 °C/min, respectively, Fig. 4. Extrapolating these temperatures to 0 °C/min [10] the transformation temperature would be

Table 1
Equilibrium phases in W series alloys, X^{α} and X^{β} are the Cr concentrations in the α and β phases of Zr

	W0.3 Zr-0.3%Cr	W1 Zr-1%Cr	W2 Zr-2%Cr	W4 Zr-4%Cr
840 °C	α + β $X^{\alpha} = 0.08$ $X^{\beta} = 1.2$	α + β + α–$ZrCr_2$ $X^{\alpha} = 0.1$ $X^{\beta} = 1.5$	α + β + α–$ZrCr_2$ $X^{\alpha} = 0.1$ $X^{\beta} = 1.5$	α + β + α–$ZrCr_2$ $X^{\alpha} = 0.08$ $X^{\beta} = 1.2$
860 °C	α + β $X^{\alpha} = 0.04$ $X^{\beta} = 0.63$	α + β $X^{\alpha} = 0.09$ $X^{\beta} = 1.13$	α + β + α–$ZrCr_2$ $X^{\alpha} = 0.16$ $X^{\beta} = 1.25$	α + β + α–$ZrCr_2$ $X^{\alpha} = 0.11$ $X^{\beta} = 1.3$
900 °C	β $X^{\beta} = 0.3$	β $X^{\beta} = 1$	β + α–$ZrCr_2$ $X^{\beta} = 1.5$	β + α–$ZrCr_2$ $X^{\beta} = 1.5$
960 °C	β $X^{\beta} = 0.3$	β $X^{\beta} = 1$	β $X^{\beta} = 2.1$	β + α–$ZrCr_2$ $X^{\beta} = 2.1$

Table 2
Equilibrium phases in N series alloys, X^{α} and X^{β} are the Cr concentrations in the α and β phases of Zr

	N0.3 Zr-0,3%Cr	N1 Zr-1%Cr	N2 Zr-2%Cr	N4 Zr-4%Cr
840 °C	α + β + α–$ZrCr_2$ X^{α} = 0.11 X^{β} = 1.2	α + β + α–$ZrCr_2$ X^{α} = 0.12 X^{β} = 1.3	α + α–$ZrCr_2$ X^{α} = 0.14	α + α–$ZrCr_2$ X^{α} = 0.16
860 °C	α + β X^{α} = 0.04 X^{β} = 1.2	α + β + α–$ZrCr_2$ X^{α} = 0.06 X^{β} = 1.04	α + β + α–$ZrCr_2$ X^{α} = 0.1 X^{β} = 1.25	α + β + α–$ZrCr_2$ X^{α} = 0.11 X^{β} = 1.3
900 °C	α + β X^{α} = 0.05 X^{β} = 0.35	β X^{β} = 1.1	β + α–$ZrCr_2$ X^{β} = 1.4	β + α–$ZrCr_2$ X^{β} = 1.4
960 °C	β X^{β} = 0.3	β X^{β} = 1	β + α–$ZrCr_2$ X^{β} = 1.9	β + α–$ZrCr_2$ X^{β} = 1.9

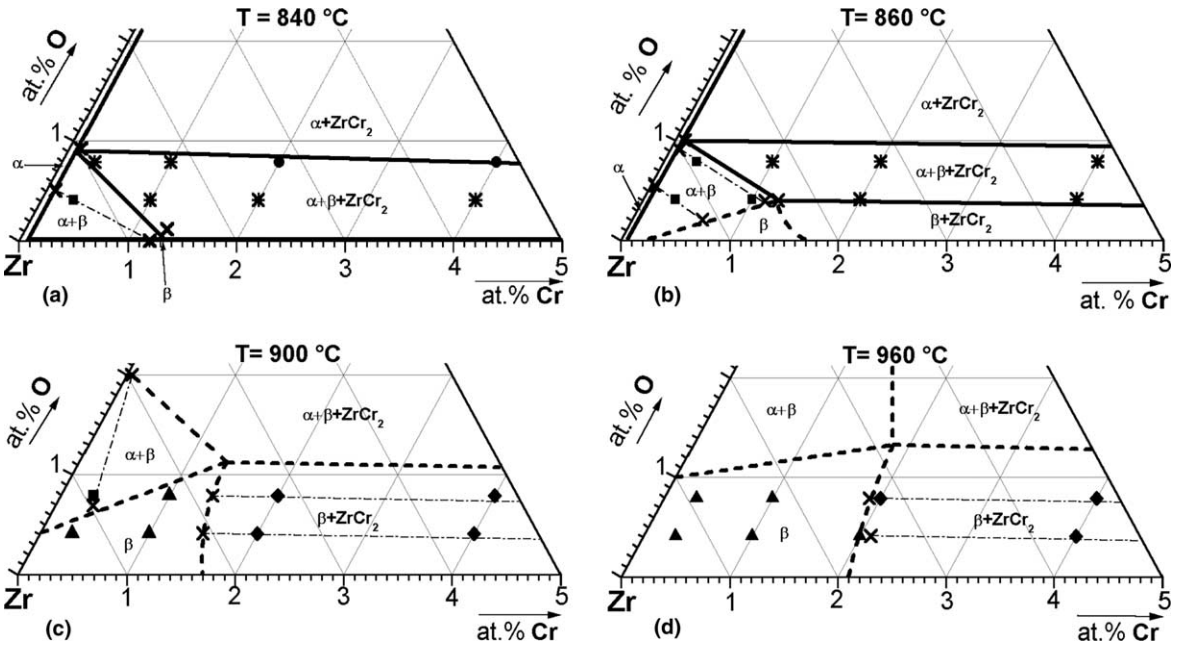

Fig. 3. Partial isotherms at 840, 860, 900 and 960 °C of the Zr–Cr–O system. (■) α + β, (✱) α + β + $ZrCr_2$, (▲) β, (♦) β + $ZrCr_2$, (●) α + $ZrCr_2$, (×—×) experimental tie-line.

Table 3
Transformation temperatures evaluated from ρ/ρ_0 vs. T curves at heating

Composition	Alloy	T (°C) at $(\rho/\rho_0)_{max}$	T (°C) at $(\rho/\rho_0)_{min}$	T (°C) at the last singularity
Zr-0.3%Cr	W0.3	830	894	–
Zr-1%Cr	W1	839	864	–
Zr-2%Cr	W2	838	862	915
Zr-4%Cr	W4	840	863	995
Zr-0.3%Cr	N0.3	832	910	–
Zr-1%Cr	N1	838	883	–
Zr-2%Cr	N2	838	869	975
Zr-4%Cr	N4	847	872	1048

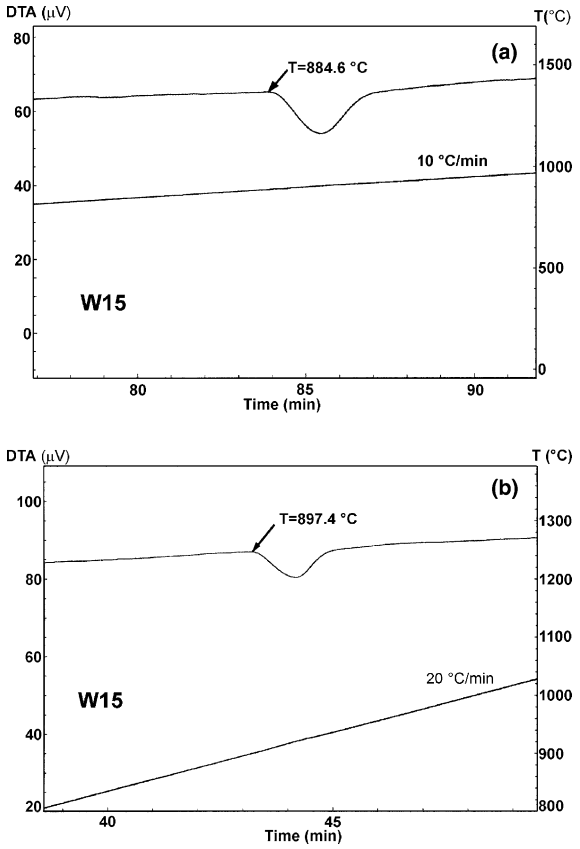

Fig. 4. DTA onset temperatures in heating at 10 and 20 °C/min.

839 °C. This value is in good agreement with the value proposed above for $T(\beta \leftrightarrow \alpha + \alpha\text{-}ZrCr_2)$.

Fig. 5 shows an isopleth section of the Zr–Cr system obtained from transformation temperatures of alloys with zirconium of nuclear purity (0.79 at.% O). Results are compared to those in [8], converted from wt% to at.%, for about 0.6 at.% O. From these compiling results and considering that the oxygen amounts in the alloys of this work has little influence in the $\alpha \rightarrow \beta$ transformation, the following reaction is suggested for the binary Zr–Cr: $\beta \leftrightarrow \alpha + \alpha\text{-}ZrCr_2$ at the eutectoid temperature $T = 840$ °C. The chromium composition of the β phase is between the 1.22 and 1.65 at.% range suggested in [8]. In the α phase it is still lower than 0.49 at.%, maximum value taken in [1]. The temperature is slightly higher than 836 °C, value mentioned in [1,2] and close to 839 °C, value calculated in [5]. Okamoto [6] comparing diagrams suggested that the one presented in [4] may be closer to the equilibrium because thermodynamic data are taken into account. The computed value for the eutectoid temperature in [4] is 836.43 °C but Okamoto, has suggested 831 °C [6].

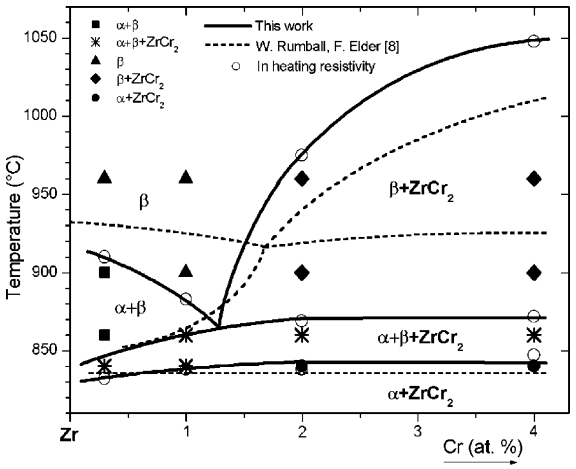

Fig. 5. Isopleth section (0.79 at.% O) of the Zr–Cr–O system as compared with the similar one in [8].

3.3. Eutectic transformation

In order to clarify the conditions of the eutectic reaction of the zone between 0 and 64 at.% Cr, W15, W26 and W26.5 alloys were studied. Microstructures of the as-cast samples of these alloys are shown in Fig. 6. It is evident that a complete eutectic structure is formed in W26.5 which induces to consider $X^L_{Cr} = 26.5$ at.%.

From EPMA measurements on the solid solution phase nearer to the intermetallic of the eutectic formed in W15 and N15 alloys (considering local equilibrium) the average composition in chromium is (4.7 ± 0.5) at.%. On the other hand, a similar amount could be validated after analyzing X-ray diffraction patterns of massive and powder samples of W26.5 alloy. The weight phase percentages were 30.4 and 69.6 for $ZrCr_2$ and β' respectively. Deducing the chromium composition in the solid solution phase from mass balances it results about 4.3 at.%. Then, $X^{\beta}_{Cr} \cong 4.7$ at.% is proposed.

Extrapolating linearly DTA results of the onset temperatures of analysis made at 10 and 5 °C/min in alloy W15 alloy to 0 °C/min, the eutectic reaction temperature is found to be 1380 °C. The conditions proposed here for the eutectic transformation $L \leftrightarrow \beta + ZrCr_2$ are $T = 1380$ °C, chromium compositions of the liquid and of the β phase, 26.5 and 4.7, respectively. These values are higher in 4.5 at.% and lower than 3.3 at.% as compared with the assessed values in [1]. The temperature is also higher in 48 °C. However, the possible influence of the oxygen composition has not been evaluated in the present work.

As a collateral result from the X-ray refinements of the diffraction patterns of W26.5 alloy, the lattice parameters of the cubic $ZrCr_2$ precipitated as a eutectic phase were $a = 0.7228$ nm and $a = 0.7222$ nm for the massive and powder sample, respectively.

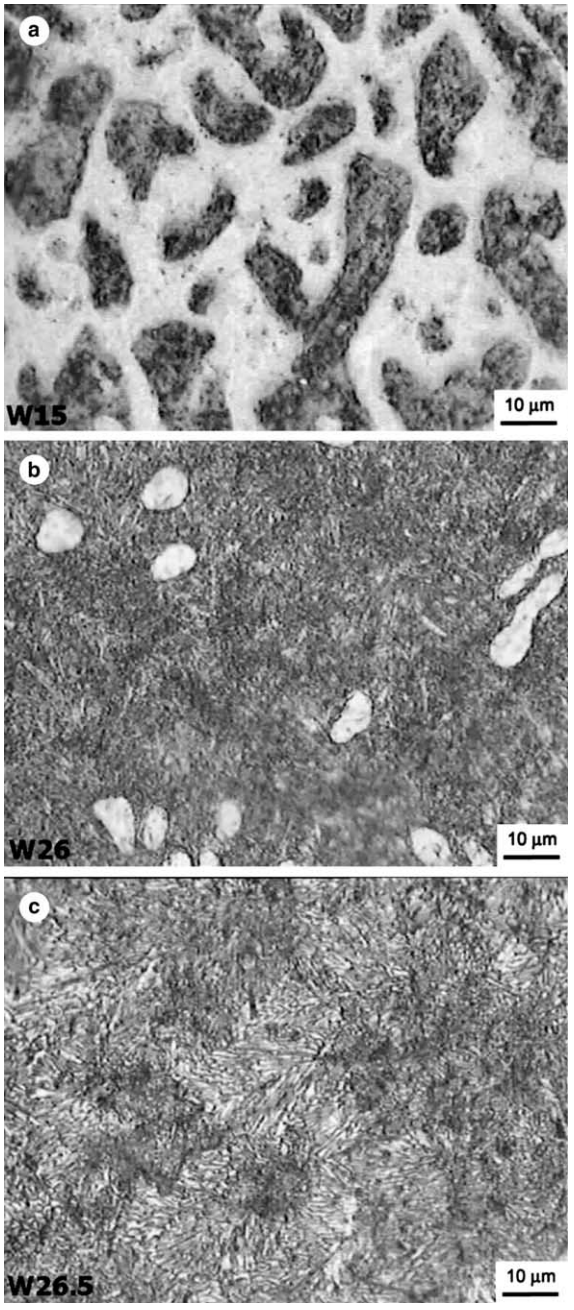

Fig. 6. As-cast microstructures of W15 (a), W26 (b) and W26.5 (c) alloys (light area is β' phase).

4. Conclusions

Some controversial zones of the zirconium–chromium diagram have been experimentally studied. The following conditions for the eutectoid and eutectic reactions are proposed:

$$\beta(X_{Cr} \sim 1.3 \text{ at.}\%) \leftrightarrow \alpha(X_{Cr} \leqslant 0.1 \text{ at.}\%) + \alpha - ZrCr_2 \quad \text{at} \quad T = 840\ ^\circ C$$

$$L(X_{Cr} = 26.5 \text{ at.}\%) \leftrightarrow \beta(X_{Cr} \sim 4.7 \text{ at.}\%) + \alpha - ZrCr_2 \quad \text{at} \quad T \sim 1380\ ^\circ C$$

The influence of oxygen in the equilibrium was generally considered, except for the eutectic temperature. Partial isothermal sections of the ternary system Zr–Cr–O in the zirconium rich zone were outlined. The lattice parameter of the cubic Laves α-$ZrCr_2$ intermetallic phase precipitated at the eutectic reaction was refined by the Rietveld method.

Acknowledgement

This work has been partially supported by grant PIP 1064/98 of CONICET (Consejo Nacional de Investigaciones Científicas y Técnicas – Argentina). Dr M. Ortiz Albuixech has analyzed X-ray diffraction patterns.

References

[1] D. Arias, J.P. Abriata, Bull. Alloy Phase Diagrams 7 (1986) 237.
[2] T.B. Massalski, H. Okamoto, P.R. Subramanian, L. Kacprzak, Binary Alloy Phase Diagrams, Second ed., ASM Publication, Ohio, 1996.
[3] L. Kaufman, H. Nesor, in: N.B. Hannay (Ed.), Treatise on Solid State Chemistry, vol. 5, Plenum Press, New York, 1975, p. 179.
[4] K. Zeng, M. Hämäläinen, R. Luoma, Z. Metallkd. 84 (1993) 23.
[5] K. Zeng, M. Hämäläinen, I. Ansara, in: I. Ansara, A. Dinsdale, M. Rand (Eds.), Thermochemical Database for Light Metal Alloys, Vol. 2, EUR 18499 EN, Luxembourg, 1993, p. 161.
[6] H. Okamoto, J. Phase Equilibria 14 (1993) 768;
H. Okamoto, Desk handbook: phase diagrams for binary alloys, ASM Publication, Berlin, 2000.
[7] S. Rhee, M. Hoch, AIME Trans. 230 (1964) 1687.
[8] W.M. Rumball, F.G. Elder, J. Less-Common, Metals 19 (1969) 345.
[9] D. Arias, L. Roberti, J. Nucl. Mater. 118 (1983) 143.
[10] Y.T. Zhu, J.H. Devletian, A. Manthiram, J. Phase, Equilibria 15 (1994) 37.
[11] W. Kraus, G. Nolze, U. Müller, Powder Cell Program, Federal Institute for Materials Research and Testing Laboratory – BAM-V-13 X-Ray Diffraction and Microanalysis, Berlin, 1998.